

Antenna and Pulse Designs for Meeting UWB Spectrum Density Requirements

Guofeng Lu, Predrag Spasojevic, and Larry Greenstein
WINLAB, ECE Department, Rutgers University
73 Brett Road, Piscataway, NJ 08854
{guofeng, spasojev, ljg}@winlab.rutgers.edu

Abstract—Antenna design in ultra-wideband (UWB) systems is a major challenge. For, in contrast to conventional systems, wherein waveform distortion by the antenna is negligible, there is potentially significant waveform distortion by UWB antennas. A further challenge to UWB system design is posed by mandated limits on power spectrum density, such as the FCC emission mask. In this paper, we join these two issues for the case of impulse radio (IR)-type UWB, showing how antenna design, transmit pulse design, filter design and attainable output signal-to-noise ratio (SNR) are intertwined. In particular, through software simulation, several antenna frequency responses are calculated, and a modified inversely-positioned bowtie antenna (‘rounded diamond’) is found to give the broadest frequency response. An integrated design of antenna, transmit pulse shaping and receive filtering is presented that gives near-maximal SNR under the FCC mask constraint, and comparisons are made to alternative designs.

I. INTRODUCTION

Ultra-wideband (UWB) [1] is an attractive technology for high data-rate indoor wireless networks. Instead of transmitting and receiving modulated sinusoidal waveforms as in carrier-based systems, a UWB¹ communication system transmits pulses which occupy several GHz of spectrum (from near DC). Therefore, UWB antennas need to be optimized for a wide range of frequencies, and pulse waveform distortion by the antennas is no longer negligible, as is reasonably assumed for carrier-based systems [2].

The half-wave dipole is a commonly used antenna in carrier-based systems. However, when a half-wave dipole pair is used for transmitting and receiving UWB signals, it is very avoid the severe ringing and dispersion problems. These are typical problems using narrow-band antenna to transmit and receive ultra-wide band pulses.

Historically, much effort has gone into designing broadband antennas such as the log-periodical, biconical, and sleeve antennas, [3], etc. There are basically two ways to make the antenna response broader: combining and smoothing. The log-periodical antenna [3] is actually a combination of dipole antennas with different lengths, and the biconical antenna forms a smooth geometry transition from the transmission line to the antenna, thereby achieving near constant impedance at

¹A UWB transmitter is defined as any intentional radiator whose fractional bandwidth exceeds 20% or whose absolute bandwidth is larger than 500 MHz. For simple presentation purposes, in this paper, we refer to UWB specifically as a single band impulse-like implementation of UWB.

all frequencies. The same applies to the broadband antenna patented by Ross [4].

None of these designs, however is suitable for modern UWB communications where small-size and low-cost (preferably system-on-a-chip) solutions are sought. Many papers have studied the behavior of simple antennas (monopole, dipole, etc.) for transmitting UWB signals (see [5]–[7]) which further strengthen the point that antenna design is a major issue for UWB communications.

This paper describes (Section II) and characterizes by simulation (Section III) a set of antennas potentially suitable for UWB communications. Then, an optimal pulse waveform synthesis for fitting the FCC mask for UWB transmissions is proposed (Section IV). Finally, signal-to-noise ratios at a matched filter output are compared for different antenna and pulse combinations (Section V). This sequence of discussions demonstrates the important interaction between pulse, antenna and filter design for UWB systems.

II. ANTENNAS CONSIDERED

We can regard the bowtie antenna (Fig. 1) as a planar version of the biconical antenna [3], as well as a planar version of the Ross antenna [4]. This two-dimensional structure is easy to place on a printed circuit board (PCB), and integrate on a chip. If we flip over the two halves of the bowtie antenna, we get a diamond (dipole) antenna [8], shown left in Fig. 2. A further improvement can be achieved by smoothing the flat bottom of the diamond antenna to obtain the rounded diamond, shown (right) in Fig. 2. The frequency responses of these planar structures are characterized by simulation next.

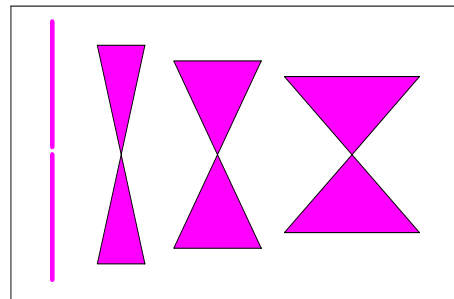


Fig. 1. Planar antennas: half-wave dipole (left) and three bowties with different expansion angles. The relative sizes are such that all antennas have a peak response at the same frequency

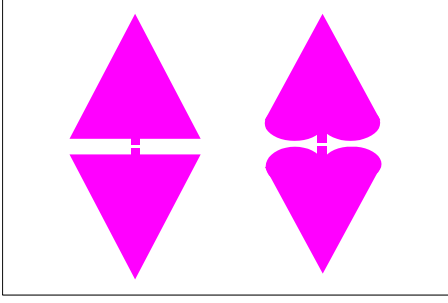


Fig. 2. Diamond antenna (left) and rounded diamond

III. SIMULATED ANTENNA FREQUENCY RESPONSES

The software packages used for simulation are the Agilent Advanced Design System (ADS), and the Remcom XFDTD. ADS is based on the Method of Moments (MoM) [9] [10], while XFDTD is based on the Finite Difference Time Domain (FDTD) method [11]. These two software packages belong to two different classes of electromagnetic analysis software, but their results are matched very well in our simulations. This establishes confidence in the validity of the results.

For comparison purposes, we assume that all antennas are sized to have a peak response at 6 GHz. The simulations assume 50-ohm source and load impedances. The frequency response obtained is the voltage transfer function (S_{21} parameter of the transmitting and receiving antenna pair) between the transmit antenna input and the receive antenna output.

Figure 3 shows frequency responses for the half-wave dipole and bowtie antennas in Fig. 1. For the bowtie antennas, we considered expansion angles of 30° , 60° , and 90° . We see that the bandwidth increases from the half-wave dipole to the broadest-angle bowtie, though not dramatically. The “signal spectrum” shown corresponds to a differentiated Gaussian pulse (or “Gaussian first derivative”), which is often used in UWB systems. Its time-domain representation and Fourier transform are:

$$p(t) = \frac{t}{\tau} \exp\left(-\frac{1}{2} \left(\frac{t}{\tau}\right)^2\right) \quad (1)$$

$$P(f) = (2\pi)^{3/2} \tau^2 f \exp\left(-\frac{(2\pi\tau f)^2}{2}\right) \quad (2)$$

The “signal spectrum” (Fig. 3) is based on having the peak response at 6 GHz, where τ is 0.0265 ns.

Simulation results for the diamond antenna and rounded diamond (Fig. 2) are shown in Fig. 4. There is a significant increase in bandwidth from the half-wave dipole to the diamond antenna. An additional bandwidth increase is achieved from the diamond antenna to the rounded diamond since the bottom rounding gives a smoother geometry transition than the original diamond. This leads to a smoother characteristic impedance and, therefore, a broader frequency response. The simulated result for the non-rounded diamond matches well with published data [8].

IV. FCC MASK AND ‘FCC PULSE’

The rounded diamond is a very broadband antenna compared with the other candidates considered above. It is still far from ideal, i.e., an ideal UWB antenna would have a flat amplitude and a linear phase response over all frequencies. However, the low-frequency falloff of actual antennas is more consistent with meeting the spectral constraints of the FCC mask (Fig. 5). The mask encourages UWB operation in the high frequency range, where the antenna is more efficient.

The ideal UWB transmission consists of sending a pulse stream which has exactly the same power spectrum density as the FCC mask, because this would yield the maximum allowable power. In Fig. 5, the FCC mask is slightly modified, i.e., the increase in allowed power spectral density below 0.95 GHz is omitted in order to avoid low-frequency content.

This modified power spectrum density can be realized using a pulse ($f_{CC}(t)$) that is a linear combination of *sinc* functions. Thus,

$$f_{CC}(t) = \sum_{i=1}^4 a_i \frac{\sin(2\pi f_i t)}{\pi f_i t}, \quad i = 1, 2, 3, 4 \quad (3)$$

where the a_i ’s are chosen so that $|F_{CC}(f)|^2$, where $F_{CC}(f)$ is the Fourier transform of $f_{CC}(t)$, has the same shape as the modified FCC mask in Fig. 5 (The pulse rate, $1/T$, affects the amplitude scaling of $|F_{CC}(f)|^2$, but we need not take this into account for present purposes). We call $f_{CC}(t)$ the *FCC pulse* and regard it as the ideal pulse shape to transmit over the air.

Since the *sinc* function is difficult to generate in practice, we have to approximate $f_{CC}(t)$ using more friendly functions. Fig. 6 (left) shows the similarity between the Gaussian second derivative and $f_{CC}(t)$ in the time domain. The Gaussian second derivative pulse is represented by:

$$x(t, \tau) = \frac{1}{\tau} \exp\left(-\frac{1}{2} \left(\frac{t}{\tau}\right)^2\right) - \frac{t^2}{\tau^3} \exp\left(-\frac{1}{2} \left(\frac{t}{\tau}\right)^2\right) \quad (4)$$

and its Fourier transform is:

$$X(f, \tau) = (2\pi)^{5/2} \tau^2 f^2 \exp\left(-\frac{(2\pi\tau f)^2}{2}\right) \quad (5)$$

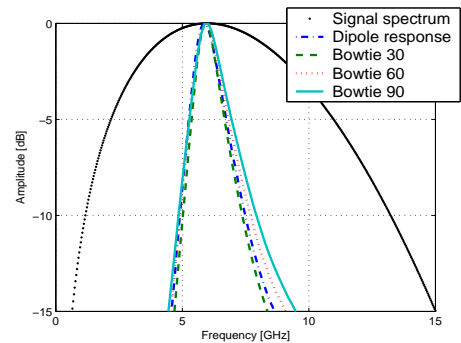


Fig. 3. Frequency responses of dipole and bowtie antennas; ‘signal spectrum’ representing a differentiated Gaussian pulse whose Fourier transform peaks at 6 GHz

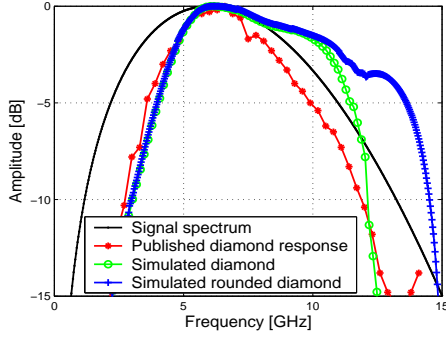


Fig. 4. Frequency response of diamond and rounded diamond antennas; ‘signal spectrum’ representing a differentiated Gaussian pulse whose Fourier transform peaks at 6 GHz; ‘published data’ is a frequency scaled-up version of data in [8]

Assuming a linear modulation scheme and i.i.d symbols, the transmitted UWB spectrum will be fully specified by the pulse spectrum [12]. If we plot the power spectrum density of $x(t, \tau)$ and the FCC mask together, we see that even though $x(t, \tau)$ and $f_{CC}(t)$ have great similarity in the time domain. The spectrum of $x(t, \tau)$ violates the FCC mask significantly, (see Fig. 6 (right)). Moreover, the violation is most severe in the GPS band.

We now seek an improved approximation to the FCC pulse. Since $f_{CC}(t)$ is a linear summation of *sinc* functions, and given the similarity between $f_{CC}(t)$ and the Gaussian second-derivative pulse, one natural extension is to use a linear combination of Gaussian second-derivatives. Therefore, a better approximation to $f_{CC}(t)$ can be written as:

$$x(t, \tau_1, \tau_2, \dots, \tau_n) = \sum_{i=1}^n b_i x(t, \tau_i) \quad (6)$$

where b_i 's are weight factors.

Any implementation of this linear combination method prefers a smaller number of component pulses, since this will relax the signal processing requirements imposed on the system. Therefore, we only use two such component pulses and define an ‘‘optimally’’ synthesized pulse using a weighted sum of two Gaussian second derivative pulses ($n = 2$), namely,

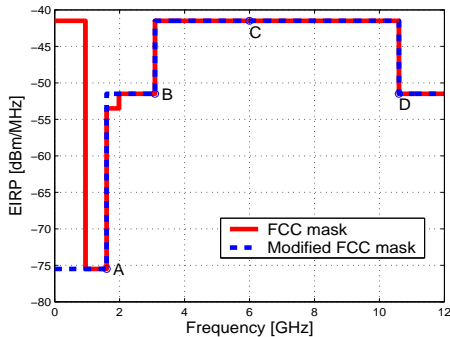


Fig. 5. FCC power spectral density constraints for indoor UWB communication device (FCC mask) and modified FCC mask

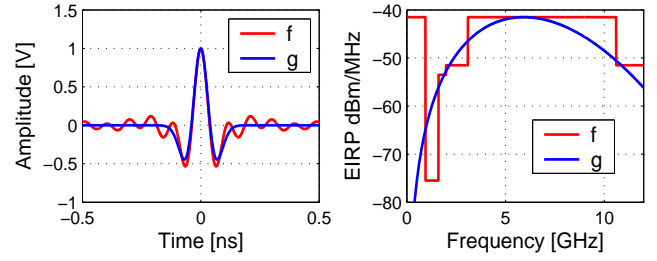


Fig. 6. Gaussian second derivative g vs. FCC pulse $f \rightarrow f_{CC}(t)$

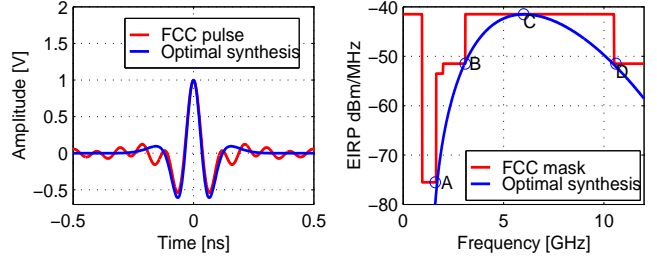


Fig. 7. Optimal synthesis of FCC pulse

the sum

$$x(t, \tau_1, \tau_2) = b_1 x(t, \tau_1) + b_2 x(t, \tau_2) \quad (7)$$

where b_1, b_2, τ_1, τ_2 are to be chosen, and $x(t, \tau)$ is given by (4). The Fourier transform of this pulse is

$$X(f, \tau_1, \tau_2) = b_1 X(f, \tau_1) + b_2 X(f, \tau_2) \quad (8)$$

The ‘‘optimally²’’ synthesized pulse is the one whose corresponding pulse stream power spectral density matches the modified FCC mask at the points A, B, D while not exceeding the horizontal line passing through point C, in Fig. 5. Our solution for this parameter set leads to the temporal and spectral comparisons shown in Fig. 7.

How to realize $X(f, \tau_1, \tau_2)$? Fig 8 shows the relevant block diagram for the transmitting end of the UWB link. In response to each data value, a Gaussian first-derivative pulse, (1), with amplitude proportional to that data value, is generated. Then, a transmit filter shapes that pulse so that the the antenna output has the desired form, $X(f, \tau_1, \tau_2)$. Thus, we require a transmit filter response of the form:

$$G_T(f) = \frac{X(f, \tau_1, \tau_2)}{P(f)H_T(f)} \quad (9)$$

where:

- $G_T(f)$ – required shaping filter response
- $X(f, \tau_1, \tau_2)$ – desired on-the-air pulse spectrum
- $P(f)$ – Gaussian first-derivative pulse spectrum
- $H_T(f)$ – transfer function of the transmitting antenna

²Another way of defining optimality is to maximize the transmitted pulse energy subject to the mask constraint. But the optimization with a constraint at every point is known to be a difficult problem to solve.

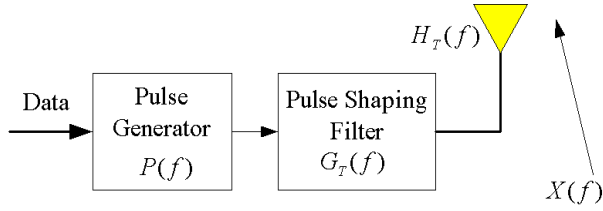


Fig. 8. Diagram for optimal synthesis

Since $X(f, \tau_1, \tau_2)$ is the weighted sum of two functions, $X_1(f, \tau_1)$ and $X_2(f, \tau_2)$, we have,

$$G_T(f) = \frac{b_1 X_1(f, \tau_1) + b_2 X_2(f, \tau_2)}{P(f) H_T(f)} \quad (10)$$

$$= \frac{b_1 X_1(f, \tau_1)}{P(f) H_T(f)} + \frac{b_2 X_2(f, \tau_2)}{P(f) H_T(f)} \quad (11)$$

$$= G_1(f) + G_2(f) \quad (12)$$

Therefore, $G_T(f)$ can be realized by two filter functions $G_1(f)$ and $G_2(f)$ in parallel, as shown in Fig. 9.

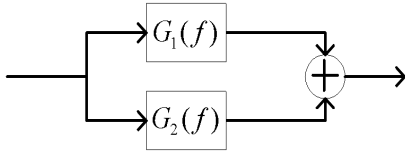


Fig. 9. Diagram for realizing the transmit shaping filter

The normalized shapes of the individual amplitude responses, $|G_1(f)|$, $|G_2(f)|$, are shown in Fig. 10. We use Figs. 9 and 10 merely to illustrate a possible method, and to show that the required filter functions are well-behaved. In practice, there are many ways to approximate the desired pulse shapes, and some of them are no doubt simpler. We also note that there are various other basic approaches for satisfying the relevant emission mask in UWB systems, e.g., [13], [14].

V. SNR RESULTS AND COMPARISONS

In the previous sections, we have identified:

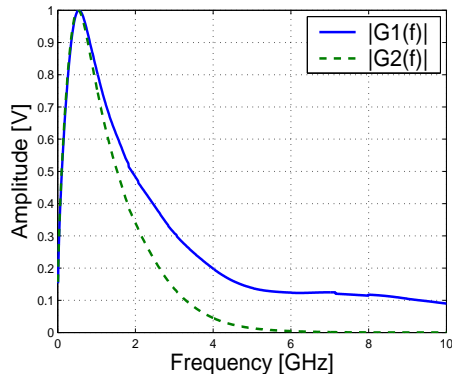


Fig. 10. Transmit filter amplitude responses

- an improved antenna (rounded diamond) for UWB
- a practical pulse shape giving us near-maximum transmitted energy while satisfying the FCC mask.

Now we would like to find out how much we gain in terms of SNR at the receiver output by using a wideband antenna and transmitting the optimally synthesized pulse. The SNR metric we use is (signal sample)²/(mean-square noise) at the detector output, assuming an isolated pulse (no inter-symbol interference (ISI)). The additional issues created by ISI, due to both filtering and multipath, are topics for further research.

The following cases are compared:

Case 1: At the transmitter, a perfect FCC pulse is radiated; at the receiver, an 'ideal' antenna is used, i.e., there is no distortion incurred by the receiving antenna. (*Ideal Case*)

Case 2: At the transmitter, a perfect FCC pulse is radiated; at the receiver, a rounded diamond antenna is used.

Case 3: At the transmitter, an optimally synthesized FCC pulse is radiated; at the receiver, a rounded diamond antenna is used.

Case 4: At the transmitter, an optimally synthesized FCC pulse is radiated; at the receiver, a half-wave dipole is used.

Case 5: At the transmitter, a Gaussian first derivative pulse is generated and is radiated by a half-wave dipole; at the transmitter, a half-wave dipole is used.

In each case, we assume that transmitting and receiving antennas have the same frequency response.

At the receiver side, all five cases use a matched filter so that, for an isolated pulse, maximum SNR is obtained. The analytical form of the SNR for each case is as follows:

$$SNR_1 = \frac{\int |F_{CC}(f)|^2 df}{N_0} \quad (13)$$

$$SNR_2 = \frac{\int |F_{CC}(f)|^2 |H_1(f)| df}{N_0} \quad (14)$$

$$SNR_3 = \frac{\int |X(f)|^2 |H_1(f)| df}{N_0} \quad (15)$$

$$SNR_4 = \frac{\int |X(f)|^2 |H_2(f)| df}{N_0} \quad (16)$$

$$SNR_5 = \frac{\int |P(f) H_2(f)|^2 df}{N_0} \quad (17)$$

where

- $X(f)$ – optimally synthesized transmit pulse spectrum
- $H_1(f)$ – diamond antenna pair voltage transfer function
- $H_2(f)$ – half-wave dipole antenna pair voltage transfer function
- N_0 – power spectral density of the white noise

Without loss in generality, we set the ideal case (*Case 1*) as our reference for comparison, since it gives the largest SNR under the FCC mask constraint. The numerical results are given in Table I.

Case 3 (an optimally synthesized FCC pulse is radiated at the transmitter; a rounded diamond antenna is used at

TABLE I
SNR LOSSES RELATIVE TO THE IDEAL CASE (*Case 1*)

<i>Case 2</i>	<i>Case 3</i>	<i>Case 4</i>	<i>Case 5</i>
-1.5 dB	-3.5 dB	-6.3 dB	-7.9 dB

the receiver) is 4.4 dB better than Case 5 (a Gaussian first derivative pulse is generated and is radiated by a half-wave dipole at the transmitter; a half-wave dipole is also used at the transmitter). The full benefit, however, is even greater, since Case 5 severely violates the FCC mask while Case 3 meets it. The 3.5 dB penalty relative to Case 1 (ideal case) reflects the impact of practical antennas (1.5 dB) and FCC pulse approximation (2 dB).

The SNR benefit of the rounded diamond antenna pair over the non-rounded pair is found to be about 0.5 dB. Additional benefits are: (1) At the transmit side, the antenna with wider bandwidth requires less emphasis of the high-frequency response in the transmit filter, simplifying its realization; and (2) at the receive side, the antenna with wider bandwidth potentially produces less ISI, simplifying the receiver design. Quantifying these benefits is a topic for further research.

VI. CONCLUSION

Our aim here has been to integrate the issues of UWB antenna and transmit pulse designs, taking into account both the stringent limits on power spectrum density and the inherent frequency selectivity of broadband antennas. Accordingly, we have (1) calculated the frequency responses of several antenna candidates; (2) derived an 'ideal' transmit pulse shape (FCC pulse); (3) devised a method for approximating this pulse shape (optimally synthesized FCC pulse); (4) computed the corresponding requirements on transmit filter response; and (5) compared relative values of attainable receiver output SNR for various antenna/pulse shape combinations. This sequence underscores the importance of considering the antenna and filter designs together in UWB systems. The final SNR comparisons, moreover, demonstrate potentially significant differences among various design choices.

In the studies performed, we have resorted to commercial software packages to estimate antenna frequency responses. For greater confidence in the overall results, the calculated antenna responses should be reinforced by measured data. Ultra-wideband measurements are in progress for several of the antennas cited here, with encouraging initial comparisons between measured and predicted responses.

VII. ACKNOWLEDGMENT

We are grateful for helpful discussions with Prof. D. Raychaudhuri, Dr. J.G. Evans, and I. Seskar.

REFERENCES

- [1] M. Z. Win and R. A. Scholtz, "Ultra-wide bandwidth (UWB) time-hopping spread-spectrum impulse radio for wireless multiple access communications," *IEEE Trans. Commun.*, vol. 48, no. 4, pp. 679–689, April 2000.
- [2] R. A. Scholtz, R. Weaver, E. Homier, J. Lee, P. Hilmes, A. Taha, and R. Wilson, "UWB radio deployment challenges," *IEEE PIMRC*, vol. 1, pp. 620–625, September 2000.
- [3] S. Silver, *Microwave antenna theory and design*, 1986.
- [4] G. F. Ross, "Transmission and reception system for generating and receiving base-band duration pulse signals without distortion for short base-band pulse communication system," U.S. Patent 3 728 632, Apr. 17, 1997.
- [5] H. F. Harmuth and D. Shao, "Antennas for non-sinusoidal waveforms. I. Radiators and II. Sensors," *IEEE Trans. Electromagn. Compat.*, vol. 25, pp. 13–24, 107–115, May 1983.
- [6] D. M. Pozar, "Waveform optimizations for Ultra-Wideband radio systems," *IEEE Trans. Antennas Propagat.*, submitted for publication.
- [7] A. Boryszenko, "Time domain studies of Ultra-wideband antennas," *Proc. of 1999 IEEE Canadian conference on electrical and computer engineering*, vol. 1, pp. 95–100, May 1999.
- [8] H. G. Schantz and L. Fullerton, "The diamond dipole: a Gaussian impulse antenna," *2001 IEEE International Sym. on antennas and propagation society*, vol. 4, pp. 100–103, Aug 2001.
- [9] K. Virga and Y. Rahmat-Samii, "Efficient wide-band evaluation of mobile communications antennas using [Z] or [Y] matrix interpolation with the method of moments," *IEEE Trans. Antennas Propagat.*, vol. 4, pp. 65–76, Jan 1999.
- [10] Agilent, *Advanced Design System 2002 manual*. Agilent Technologies Inc, 2002.
- [11] K. Luebbers, *The finite difference time domain method of electromagnetics*, 1993.
- [12] J. G. Proakis, *Digital Communications, Fourth edition*. Columbus, OH: McGraw-Hill Companies, Inc, 2001.
- [13] Y.-P. Nakache and A. F. Molisch, "Spectral shape of UWB signals—influence of modulation format multiple access scheme and pulse shape," *VTC-F '03*, 2003, to appear.
- [14] W. Yu, A. F. Molisch, S.-Y. Kung, and J. Zhang, "Impulse radio pulse shaping for ultra-wide bandwidth (UWB) system," *PIMRC '03*, 2003, to appear.